ICES Journal of Marine Science

ICES Journal of Marine Science (2017), 74(4), 1125–1134. doi:10.1093/icesjms/fsx017

Contribution to Special Issue: 'Towards a Broader Perspective on Ocean Acidification Research Part 2'

Original Article

Effects of current and future coastal upwelling conditions on the fertilization success of the red abalone (*Haliotis rufescens*)

Charles A. Boch[1,2,*], Steven Y. Litvin[2], Fiorenza Micheli[2], Giulio De Leo[2], Emil A. Aalto[2], Christopher Lovera[1], C. Brock Woodson[3], Stephen Monismith[4], and James P. Barry[1]

[1]*Monterey Bay Aquarium Research Institute, 7700 Sandholdt Road, Moss Landing, CA 95039, USA*
[2]*Hopkins Marine Station, Stanford University, Pacific Grove, CA 93950, USA*
[3]*College of Engineering, University of Georgia, Athens, GA 30602, USA*
[4]*Department of Civil and Environmental Engineering, Stanford University, Stanford, CA 94305, USA*

**Corresponding author: tel: 831-775-1849; fax: 831-775-1620; e-mail: cboch@mbari.org*

Boch, C. A., Litvin, S. Y., Micheli, F., De Leo, G., Aalto, E. A., Lovera, C., Woodson, C. B., Monismith, S., and Barry, J. P. 2017. Effects of current and future coastal upwelling conditions on the fertilization success of the red abalone (*Haliotis rufescens*). – ICES Journal of Marine Science, 74: 1125–1134.

Received 30 August 2016; revised 10 January 2017; accepted 29 January 2017; advance access publication 30 March 2017.

Acidification, deoxygenation, and warming are escalating changes in coastal waters throughout the world ocean, with potentially severe consequences for marine life and ocean-based economies. To examine the influence of these oceanographic changes on a key biological process, we measured the effects of current and expected future conditions in the California Current Large Marine Ecosystem on the fertilization success of the red abalone (*Haliotis rufescens*). Laboratory experiments were used to assess abalone fertilization success during simultaneous exposure to various levels of seawater pH (gradient from 7.95 to 7.2), dissolved oxygen (DO) (~60 and 180 μm·kg SW) and temperature (9, 13, and 18 °C). Fertilization success declined continuously with decreasing pH but dropped precipitously below a threshold near pH 7.55 in cool (9 °C—upwelling) to average (13 °C) seawater temperatures. Variation in DO had a negligible effect on fertilization. In contrast, warmer waters (18 °C) often associated with El Niño Southern Oscillation conditions in central California acted antagonistically with decreasing pH, largely reducing the strong negative influence below the pH threshold. Experimental approaches that examine the interactive effects of multiple environmental drivers and also strive to characterize the functional response of organisms along gradients in environmental change are becoming increasingly important in advancing our understanding of the real-world consequences of changing ocean conditions.

Keywords: climate change, fertilization, *Haliotis rufescens*, hypoxia, multiple drivers, ocean acidification, ocean warming, upwelling.

Introduction

Fossil fuel CO_2 emissions are driving massive and rapid changes in global temperature and ocean chemistry (Bakun, 1990; Caldeira and Wickett, 2003; Sabine *et al.*, 2004; Solomon *et al.*, 2007; Chan *et al.*, 2008). These global scale impacts are leading to a cascade of changes in ocean stratification, transport, convection, and other key processes at both regional and local scales. In the California Current Large Marine Ecosystem (CCLME), shoaling of the oxygen minimum zone (Stramma *et al.*, 2010) has promoted a reduction in the pH and dissolved oxygen (DO) content of upwelled waters that are advected into nearshore habitats (Chan *et al.* 2008; Feely *et al.*, 2008; Bograd *et al.*, 2008; Connolly *et al.*, 2010; Keeling *et al.*, 2010; Deutsch *et al.*, 2011; Booth *et al.* 2012; Walter *et al.* 2014). In addition, an increase in El Niño-like conditions in combination with global ocean warming has resulted in recent increases in temperatures in coastal ecosystems of the CCLME (Trenberth and Hoar, 1997; Lee and McPhaden, 2010; Cai *et al.*, 2014). These growing changes in key ocean conditions are predicted to directly affect the physiology of many marine organisms, with potentially profound effects on the sustainability of marine populations (Vaquer-Sunyer and Duarte, 2008; Portner and Farrell, 2008; Somero *et al.*, 2016). To date,

however, most research has focused on the response of marine organisms to shifts in a single oceanographic parameter (reviewed by Gattuso *et al.*, 2015) and our understanding of biological responses to simultaneous changes in multiple ocean conditions is poorly understood. Experimental approaches that assess the response of species, assemblages, and marine communities to realistic future environmental variation among multiple drivers (e.g. Kroeker *et al.*, 2013) are needed to refine our ability to predict the future stability of ecosystem function and the sustainability of ocean-based economies (Gattuso *et al.*, 2015).

The persistence of natural populations depends on successful reproduction, and much research has focused on the effects of ocean acidification, hypoxia and temperature variation on fertilization success and early development in marine species (reviewed by Byrne, 2011). Although several biological factors (e.g. gamete concentration, sperm:egg ratios, gamete age; Babcock and Keesing, 1999; Baker and Tyler, 2001; Huchette *et al.*, 2004) or changes in ocean conditions (e.g. pH; Kurihara and Shirayama, 2004; Havenhand *et al*, 2008) are known to affect fertilization success, few studies have examined the effects of simultaneous exposure to multiple environmental changes (e.g. Byrne *et al*, 2010). Thus, we are just beginning to address how simultaneous exposure to multiple drivers may influence these key processes in marine organisms, and importantly, whether non-linear responses and tipping points exist across chemo-physical drivers. These questions are particularly relevant in systems where environmental conditions are highly variable in space and time, and where this variability is predicted to increase under future climate change scenarios, such as upwelling ecosystems (Bakun, 1990; Sydeman *et al.*, 2014; Bakun *et al.*, 2015). Here, we addressed the individual and interactive effects of current and expected future pH, DO, and temperature on fertilization success using a nearshore benthic invertebrate, the red abalone *Haliotis rufescens*, as a model system. Red abalone (*H. rufescens*), naturally inhabit the intertidal to a depth of ca. 30 m from Southern Oregon to Central Baja California of the CCLME (Booloottian *et al.*, 1962).

Abalone and other ecologically important and economically valuable benthic invertebrates are unable to escape bottom hypoxia because of their limited mobility. They are also are negatively affected by high pCO_2 (low pH) that can interfere with shell deposition and growth, and are impacted by high temperatures, directly or indirectly, through the loss of their algal food resources (Shepherd *et al.*, 1998; Orr *et al.*, 2005; Micheli *et al.*, 2012; Gazeau *et al.*, 2013; Kim *et al.*, 2013). The question of how different combinations of drivers may independently or interactively affect abalone and other species remains unanswered. However, recent experiments indicate that exposure to even a limited range of low pH and low DO may have deleterious effects on mortality and growth of early stage of red abalone juveniles (Kim *et al.*, 2013). Therefore, to increase our understanding of the likely future effects of climate-driven changes in ocean conditions for marine species, it is crucial to explore the effects of simultaneous exposure to key environmental variables on critical processes such as fertilization.

Here we examined the effects of variation in seawater pH, DO, and temperature on the fertilization success of red abalone *H. rufescens*. These oceanographic parameters are highly variable in upwelling affected areas of nearshore habitats in the CCLME, and their range of variability is shifting in response to climate change (Sydeman *et al.*, 2014) and as such, future upwelling is expected to be increasingly stressful for coastal species (Somero *et al.*, 2016). We employed a hybrid (regression/factorial) experimental approach to assess abalone fertilization success across a gradient of seawater pH (regression, 40+ pH levels), combined with a factorial approach for DO (two levels: 6 and 2 mg/l DO) and temperature (three levels: 9, 13, and 18°C). This novel hybrid design allowed us to characterize the functional response of fertilization over a large range of pH, under multiple co-varying conditions, and assess potential thresholds to changes in pH beyond current day variation.

Based on previous studies, we hypothesized that decreasing pH may have a negative effect on fertilization (Kroeker *et al.*, 2010; Gazeau *et al.*, 2013). However, potential interactions with DO and temperature were difficult to predict because of the limited range or the number of pH levels that have been previously examined (Byrne *et al.*, 2010). While decreasing pH may reduce fertilization success, an additional driver may not further affect fertilization or the independent effects of a secondary driver may dominate, thus decoupling fertilization success from the effects of pH (dominant stressor model; Halpern *et al.*, 2008). In a more complex process, a secondary driver may interact with pH, modifying the decline in fertilization rates along the pH gradient by ameliorating or exacerbating negative impacts (antagonistic and synergistic effects, respectively; Crain *et al.*, 2008). Finally, the effects of an additional environmental driver may be non-linear along a pH gradient.

Methods

Preparation of seawater treatments

Two days before each experiment, seawater sources were produced using the nitrogen, air, and CO_2 gas control system described in Barry *et al.* (2008) and stored at 13°C in gas-tight 10 l mylar bags (Calibrated Instruments, Inc., NY, USA) with one-way Luer Lock stopcocks. The target pH (total scale) and DO concentration of the seawater sources (Supplementary Table S1) were adjusted in order to achieve the ranges utilized in the fertilization experiments (pH 7.95–7.2 and DO 6 and 2 mg/l) while accounting for the process of adding gametes (see 'Assessment of fertilization success' section below). After 24 h, pH (n = 3 each; UV-1601 spectrophotometer, Shimadzu, Kyoto, Japan) and total alkalinity (n = 8; TA, TitroLine 7000 open cell, potentiometric titration system, SI Analytics, Germany) of each seawater source were measured and used to estimate dissolved inorganic carbon concentrations (DIC, at 13°C and 33 psu). In addition, DO concentrations were verified using an Aanderaa 3830 optode (Xylem Inc., NY, USA). Based on DIC and TA values (Supplementary Table S1 and S2), mixtures of each seawater source needed to achieve the desired range of pH and DO for a particular experiment (see Supplementary material 'Preparation of seawater sources and Determination of volumetric mixtures of seawater sources to achieve target pH and DO' section) were determined using CO_2SYS (http://cdiac.ornl.gov/oceans/co2rprt.html). These predetermined mixtures were then loaded into 50 ml gas-tight glass syringes fitted with three-way Luer Locks ("experimental syringes"; Tomopal, Japan). To remove any bubbles, 15 ml of seawater was extruded and the syringe re-sealed, retaining 35 ml of treatment seawater. Syringes were then stored overnight in a temperature controlled seawater baths appropriate for the given experiment (8.5, 13, or 18.5°C, see description of experiments below). In preliminary studies, we determined that the change in

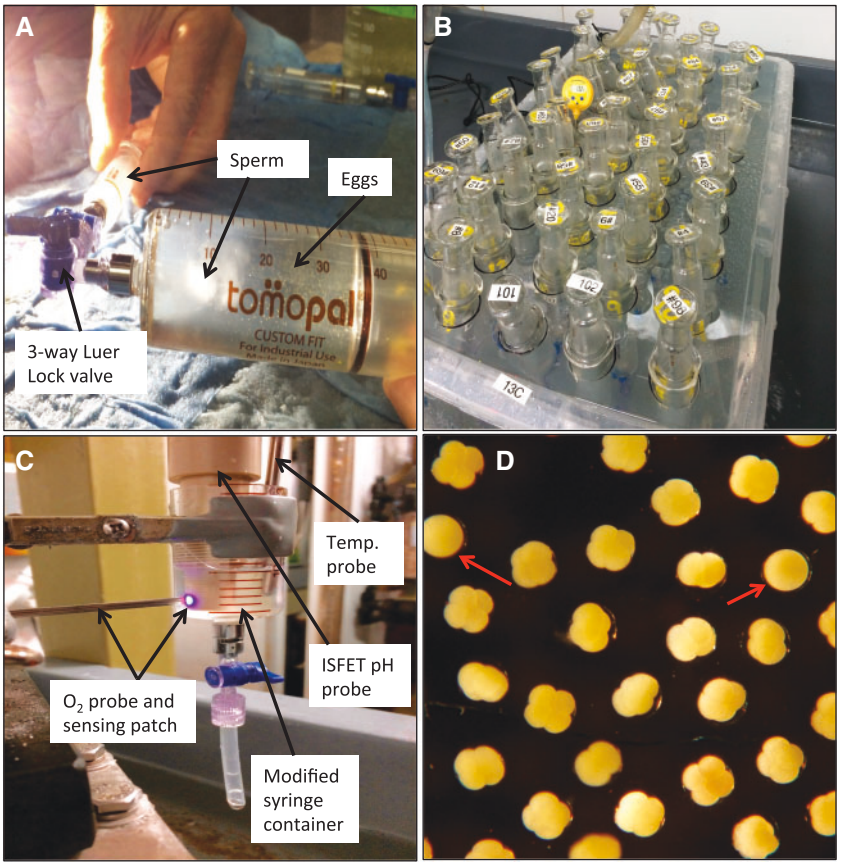

Figure 1. General procedure during the fertilization experiments. **A**. Known concentrations of sperm (white cloud) are loaded after egg injection (white flecks) into 50 ml gas-tight syringes (Tomopal, Japan) with specified pH, DO, and temperature levels. Seawater is kept water tight in syringes with 3–way Luer Lock valve and connector. **B**. A final 1 ml of seawater is injected into the syringes to flush any gametes in the valves. Then all the syringes are incubated for 600 seconds in the appropriate temperature tank. **C**. 20 ml out of the total 40 ml in each syringe are loaded into a modified 50 ml syringe container to measure the pH (SentrON-Line 8100-100 ISFET probe connected by RS232 cable to a logging computer), dissolved oxygen and temperature (NeoFox hyoxy probe, sensing patch and temperature probe connected via USB to a logging computer). **D**. Sample micrograph showing unfertilized eggs (single cells indicated by red arrows) and 4-cell stage fertilized eggs (remainder of the cells) after 600 seconds of treatment followed by 4-hours of incubation at non-stressful levels.

carbonate chemistry and DO within experimental syringes was negligible over several days.

Abalone spawning, gamete concentration determination, and gamete density adjustment

Abalone were obtained from American Abalone Farms, Davenport, CA, USA. For each experiment, six males (mean shell length = 86.4 mm ± 4.0 *SD*) and six females (mean shell length = 94.5 mm ± 5.8 *SD*) were conditioned in two tanks with flowing 13°C seawater, 0:24 Light:Dark photoperiod, and fed giant kelp, *Macrocystis pyrifera*, *ad libitum* for 2 weeks prior to the day of experiment. On the day of each experiment, we separated the male and female brooders into individual induction containers and used the tris-buffer, hydrogen peroxide, and temperature protocol to individually induce spawning (Morse *et al.*, 1977). We delayed the initiation of the protocol for males by ~1.5h, relative to females, in order to synchronize spawning between sexes. Over the experiments, 95% of male and female abalone spawned within a 1-h window.

Upon commencement of spawning, sperm and eggs from all spawning individuals were pooled in separate 500 ml, autoclaved glass beakers. Gamete collection was limited to 45 min after the first animal spawned to reduce the potential effects of gamete age on fertilization success. To determine initial density of the pooled sperm stock, micrographs of sperm stained with Lugol's solution were taken on a hemocytometer (Bright-Line, PA, USA) with an Axioscop compound microscope (10×, Zeiss, Germany, Olympus ZH71 camera attachment and CellSens software). ImageJ (https://imagej.nih.gov/ij/) software was then used to automatically enumerate sperm (n = 2 samples from pooled sperm stock, see Supplementary material 'Estimation of sperm density via image analysis' section and Supplementary Figures S1A–C). To estimate initial egg density, the number of eggs in 50 µl (n = 4) subsamples of the pooled egg stock were counted on an Olympus SZH10 dissecting microscope. From these estimates and accounting for the process of adding gametes into seawater treatments (final volume of 40 ml in each syringe, see 'Assessment of fertilization success' section below), sperm and egg stock densities were diluted with control sea water to achieve a final concentration of sperm and eggs in each syringe of 10^6 and ~60 ml^{-1}, respectively (see Supplementary material 'Determination of experimental sperm density and exposure time' section). During and after density adjustments, gamete stocks were maintained at 13°C.

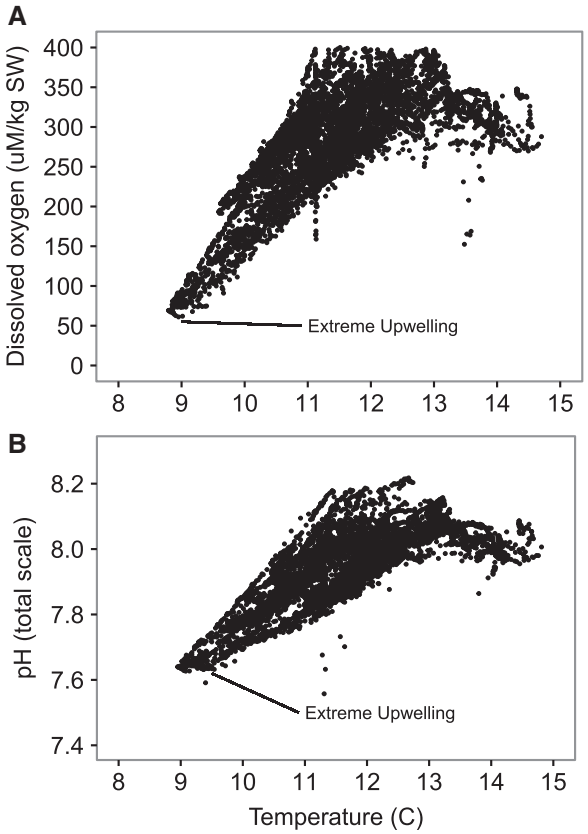

Figure 2. pH, dissolved oxygen, and temperature (1 m above the bottom, 25 April, 2013 – 14 June, 2013) from a near shore upwelling zone (~6 m depth; 36.624 °N; 121.905 °W). **A**. pH (total scale) versus temperature (SeaFET pH sensor, Satlantic, Halifax, Canada). **B**. Dissolved oxygen versus temperature (SBE 16 CTDO, Sea-Bird Electronics, Inc., Washington, USA). The extreme pH and dissolved oxygen and associated temperature during upwelling at this site are noted in both panels.

Assessment of fertilization success

To access fertilization success, sperm and eggs from the adjusted density pooled gamete stocks were injected into 50 ml experimental syringes pre-loaded with volumetric mixtures of seawater sources (see 'Preparation of seawater treatments' section above) to achieve the range of pH and DO for a given experiment and held at the appropriate temperature (8.5, 13, or 18.5°C, see description of experiments below). A 2 ml of egg stock solution, followed by 2 ml of sperm stock solution, were injected into the experimental syringe using separate 5ml gas-tight syringes with one-way Luer Locks (Figure 1a). Subsequently, 1 ml of control seawater was injected from a separate 5 ml syringe to flush any gametes remaining in the Luer Lock into each experimental syringe (see Supplementary Tables S1 and S2 for final flush source), bringing the final total volume to 40 ml. The order which experimental syringes were inoculated with gametes was randomized with the exception of controls (see descriptions of experiments below), which were conducted at the start, finish and across regular intervals during each experiment.

After gamete injection, each experimental syringe was held in a second temperature bath (Figure 1b, 9, 13, or 18°C, see description of experiments below) and eggs were exposed to sperm for a duration of 600 s (see Supplementary material 'Determination of experimental sperm density and exposure time' section). Subsequent to the exposure period, 20 ml of each experimental syringe was expunged into a 50 ml falcon tube, with the bottom removed and replaced with Nitex 90 µm mesh, then immersed repeatedly in control seawater (pH ~7.95, DO ~6.0 mg/l, 13°C) to wash away excess sperm and terminate the exposure period. Each tube was held in bins filled with flowing control seawater for 4 h, at a depth that maintained each tube approximately two-third filled, to allow fertilized eggs to develop. Samples were then washed into 20 ml glass scintillation vials and fixed with 500 µl of 10% formalin. For each sample, >100 cells were examined using an Olympus SZ40 dissecting microscope to access proportional fertilization success, with eggs reaching a two-cell stage or greater counted as fertilized (Figure 1d).

Measurement of post-fertilization experimental syringe pH and DO

The remaining 20 ml of sample was held in the sealed experimental syringe (<3 h) at 13°C until pH and DO were measured. A SentrON-Line 8100-100 ISFET probe (Sentron, NL) was used to estimate pH (total scale) and a NeoFox spectrometer (OceanOptics, FL, USA) system to measure DO and temperature (Figure 1c, for details see supplementary material 'Determination of post fertilization experimental syringe pH and DO' section).

Effects of ocean acidification and hypoxia on fertilization rates

The range of current environmental variability along the central California coast within the CCLME was used to determine the range of treatments levels for pH, DO, and temperature over which abalone fertilization success was measured. Records of temperature, DO, and pH from a depth of 6 m off Hopkins Marine Station were made during the spring upwelling period (observations in April–June, 2013 season) (Figure 2), indicating extremes during upwelling conditions of pH 7.5, DO 60 µmol/kg SW (approximately 2.0 mg/l DO), and 9°C. Although it is difficult to predict the time scales and magnitude of changes in the composition of upwelled waters in response to rising atmospheric CO_2 (Feely *et al.*, 2004, 2008) we used a pH offset of -0.3 pH (reference for global surface water pH change) units below the current upwelling minimum as a pH minimum (7.2) for our experiments. Thus, to assess the effects of current upwelling conditions, as well as scenarios reflecting future acidification and deoxygenation, we evaluated fertilization success across 40 levels of pH ranging from ~7.95 to ~7.2 pH crossed with two DO concentrations representing normoxic and hypoxic conditions (5.7 and 1.97 mg/l DO, respectively) at 13°C.

Effects of acidification and ocean warming on fertilization rates

To assess the effects of pH and temperature typical for present-day upwelling (Figure 2b, pH 7.5, 9°C) and future ocean acidification and warming scenarios (pH 7.2–7.5, 18°C), we evaluated fertilization success across a range of pH, ~7.95 to ~7.2 pH, across two temperatures (n = 45 for 9 and 18°C). It is important to note that experimental syringes were stored at 8.5, and 18.5°C overnight prior to inoculation (see 'Preparation of seawater treatments' section) in order to achieve targeted temperatures (9, and

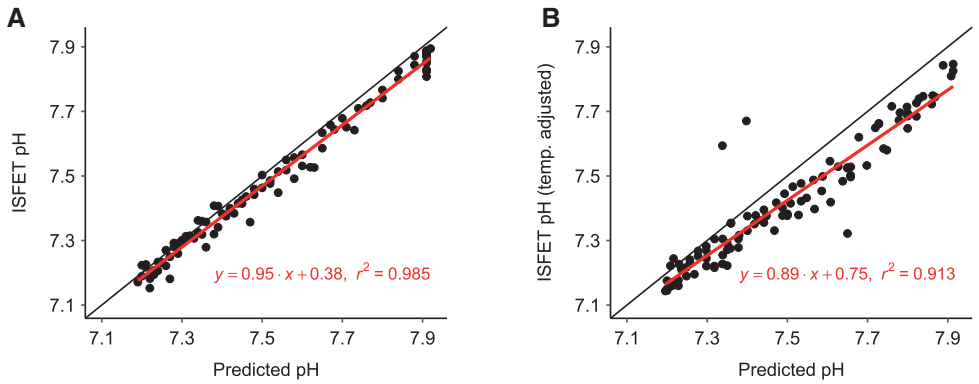

Figure 3. Measured *vs*. predicted pH. **A**. Correlation between SentrOn-Line 8100-100 ISFET probe (ion-sensitive field-effect transistor; Sentron, Netherlands) measured pH output (total scale) versus CO2Sys predicted pH (total scale) from source water mixing at 13 °C. **B**. Correlation between SentrOn-Line 8100-100 ISFET probe (ion-sensitive field-effect transistor; Sentron, Netherlands) measured pH output (*y*-axis) versus CO2Sys predicted pH from source water mixing for 9, 13, and 18 °C. **For both panels**, open circles represents each sample treatment from the experiment (n=92 and n=108 respectively). Dashed line is the linear regression line fit and the solid black line represents 1 to 1 unity. SentrON-Line 8100-100 probe was connected via RS232 cable to a PC and the data logged via DataLogger Suite software.

Table 1. Dissolved oxygen and temperature measurements from experimental treatments.

Experiment	Group	n	mean	SD	SE
A. Ocean acidification and hypoxia	Control	12	5.70	0.35	0.10
	Low DO	40	1.97	0.33	0.05
	High DO	40	5.72	0.35	0.06
B. Ocean acidification and warming	Control	5	13.56	0.06	0.11
	Low Temp.	5	9.30	0.25	0.02
	High Temp.	4	17.90	0	0

n = number of samples. Dissolved oxygen (mg/l) during experiment A was measured using NeoFox Hyoxy dissolved oxygen sensor (OceanOptics, FL, USA). Temperature (°C) during experiment B was measured using Taylor Digital Probe Thermometer 9842 (Taylor Precision Products, New Mexico, USA). Temperature samples were taken every 20 minutes over ~80 minutes (the full duration of experiment B).

18°C, respectively) while accounting for the temperature of the seawater used in the process of adding gametes (13°C). Subsequently, experimental syringes were held at 9 and 18°C (Figure 1b), as appropriate, during the period of gamete exposure (600 s).

Statistical analysis

To evaluate proportional fertilization success as a function of measured pH in combination with DO or temperature groups, response data were logit transformed and evaluated for any significant response to pH, DO, and temperature using Generalized Linear Models (GLMs) in R (Warton and Hui, 2011). Homogeneity of the data was assessed via visual inspection of residuals versus GLM predicted logit transformed data (Supplementary Figure S3). These GLM models were then incorporated into Segmented Model analysis to determine the existence of a threshold or a breaking point, and any changes in the response slopes as a function of pH and any additional factors (Muggeo, 2003, 2008). Additional comparison of GLM and Segmented Model fits were assessed using corrected Akaike Information Criterion (AICc) with a reduction of AICc > 10 by the Segmented Model used as a conservative estimate for reporting a significant improvement relative to the GLM and further evidence for non-linearity and a possible threshold.

Results

Seawater treatment measurements

Overall, the mean difference between predicted pH and measured pH was 0.03 ± 0.03 pH units for the ocean acidification and hypoxia experiment and 0.08 ± 0.06 pH units for the ocean acidification and ocean warming experiment. For the former experiment, the mean DO for the control group was 5.70 ± 0.35 mg/l DO, 5.72 ± 0.35 mg/l for the High DO group, and 1.97 ± 0.33 mg/l for the hypoxic Low DO group. For the latter experiment, the temperature in the incubation bins during the fertilization time remained stable at 13.6, 9.3, and 17.9°C for the Control, Low, and High Temperature groups (Table 1). Measured pH showed a high correlation with predicted pH values from CO_2SYS for both experiments with r^2= 0.99 and r^2 = 0.91 (Figure 3a and b). The lower r^2 value in the second regression experiment is attributed to 3 pH outliers that were likely caused by inconsistent volume mixture during preparation.

Fertilization response to ocean acidification and hypoxia

Overall, fertilization success decreased from ~59 to 4% as pH decreased from 7.9 to 7.18 for the low DO group (~1.97 mg/l DO). For the normoxic group (~5.72 mg/l DO), fertilization dropped from 58 to 3% as pH decreased from 7.84 to 7.15. In the control group (7.81–7.89 pH, ~5.70 mg/l DO), fertilization success ranged from 59 to 38%. These results are shown in Figure 4a. Results of the GLM model (Table 2, Model A) showed that the pH × DO interaction was not significant, indicating that DO did not interact with pH to affect variation in fertilization success. Further evaluation with Segmented Model analysis revealed a significant threshold at a pH of 7.56 (±0.03 SE) and a significant change in the intercept and slope below this threshold estimate [Table 3(A)]. These results indicate a greater drop in fertilization success per unit of pH change below this point. AICc comparison

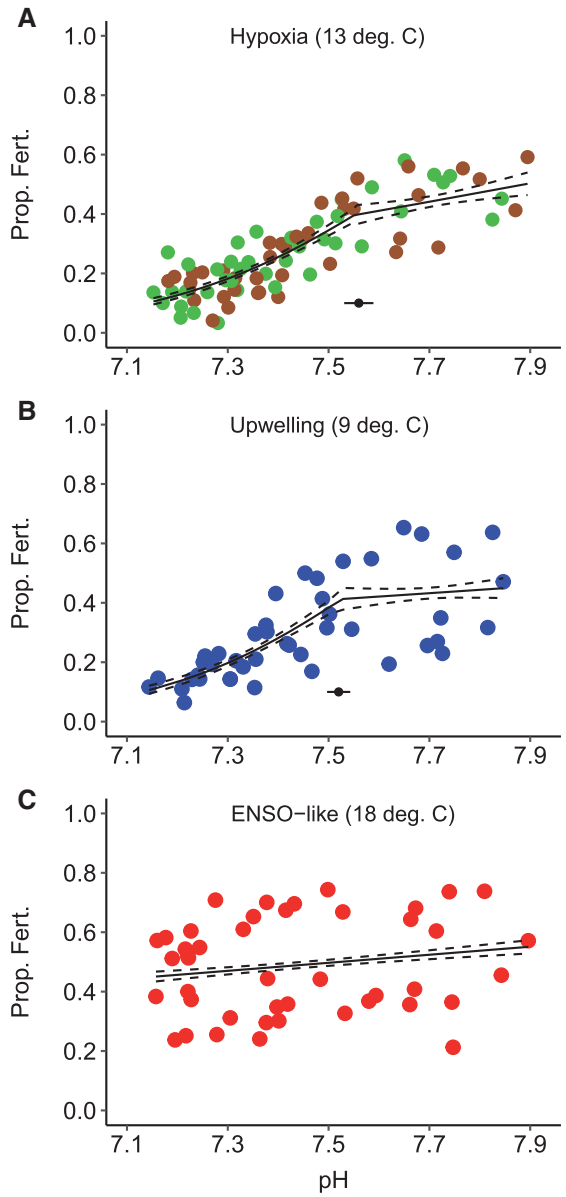

Figure 4. Abalone fertilization response to multiple stressors. **A.** Open circles represent proportional fertilization at pH (total scale) ranging from ~7.9 to ~7.2 and 6.0 mg/l dissolved oxygen. Black solid dots represent responses to pH ranging from ~7.9 to ~7.2 and 1.5 mg/l dissolved oxygen. For all the treatments in this experiment, temperature was maintained at 13 °C. Solid black line represents segmented model fit with dashed lines representing lower and upper 95% confidence limits. **B.** Proportional fertilization success (solid blue circles) to pH ranging from ~7.9 to ~7.2 and 9 °C. Solid black line represents segmented model fit with dashed lines representing lower and upper 95% confidence limits. **C.** Proportional fertilization success (squares) to pH ranging from ~7.9 to ~7.2 and 18 °C. Solid black line represents GLM fit with dashed lines representing lower and upper 95% confidence limits. For panels B-C, dissolved oxygen was maintained at normoxic levels. **For all panels**, *y*-axis represent proportional fertilization success and *x*-axis represent the measured pH in each experimental sample (n=92 for C and n=108 for C). For panels A and B, black solid circles represent break-point estimates with error bars.

of GLM with Segmented Model fits showed that the Segmented Model was a significant improvement over the GLM (SM, Table 3, AICc > 10) indicating a non-linear response of fertilization success to decreasing pH.

Fertilization response to ocean acidification and warming

Similar to the ocean acidification and hypoxia experiment at 13°C, fertilization rates decreased with decreasing pH when gametes were exposed to the upwelling-like temperature of 9°C (Figure 4b). At 9°C, fertilization decreased from ~65 to 6% as pH decreased from 7.85 to 7.14, with the Segmented Model analysis indicating a threshold at a pH of 7.52 (±0.02 SE), below which with a much steeper reduction in fertilization occurred. In contrast to 9 and 13°C treatment and an equivalent range of pH exposure, fertilization success decreased from ~74 to 21% as pH decreased from 7.95 to 7.1 at 18°C (Figure 4c). The results from the GLM evaluation showed a significant increase in the intercept and a decrease in the slope when the 18°C exposure interacts with the range of pH examined (Table 2B, $p < 0.001$). Further evaluation with the Segmented Model analysis showed a lack of breaking point or a significant change in the intercept and slope at the warmer temperature [Table 3(C)] thus indicating the linear prediction evaluated by GLM model is an appropriate predictor of fertilization rates at this temperature. AICc comparison of GLM with Segmented Model fits showed that the Segmented Model was not a significant improvement over the GLM predictions supporting the results of the Segmented Model analysis (Supplementary Table S3, AICc < 10).

Discussion

This is the first evidence of direct and interactive effects of variation in pH, DO and temperature on fertilization success in red abalone. Specifically, the results indicate that: (i) fertilization generally decreases with declining pH, with the presence of a threshold and the difference in the rate of change in fertilization success dependent on the temperature and pH interaction; (ii) warming above ambient temperature interacts with pH, and ameliorates the negative impact of low pH; (iii) DO has no discernable effect on fertilization success, at least within the range of oxygen variation investigated in this study.

Both negative and resistance to low pH on marine invertebrate fertilization success have been reported in the literature but these diverse outcomes are likely due to the range of pH examined and to the limited understanding of the fertilization mechanism that is being affected. Similar to our study, reductions in fertilization success with decreasing pH have been reported for several species of molluscs and echinoderms (Kurihara and Shirayama, 2004; Moulin *et al.*, 2011; Barros *et al.*, 2013; Frieder, 2014; Scanes *et al.*, 2014). In these studies, low fertilization success was evident as gametes were exposed to pH levels below 7.6. In contrast, fertilization success remained high with decreasing pH for echinoderms (*Heliocidaris tuberculata, Heliocidaris erythrogramma, Tripneuestes gratilla, Centrostephanus rodgersii, Patirriella regularis*) and the abalone *Haliotis coccoradiata* (Byrne *et al.*, 2010). Although fertilization success in these organisms was found to be resistant when exposed to pH levels ranging from 8.2 to 7.6, the authors suggested that this resistance might change under more severe levels of pH. In a mechanistic context, these previous studies suggested

Table 2. Statistical results for proportion fertilized in each experiment.

Model		Estimate	SE	*z*-value	*p*-value
A. Model for pH and DO experiment:	(Intercept)	−24.69	1.16	−21.22	***
y = pH + DO Group + pH * DO Group + e	pH	3.19	0.16	20.41	***
	Low DO	1.66	1.61	1.03	NS
	pH x Low DO	−0.23	0.22	−1.07	NS
	Null Deviance:	1316.42 (79 d.f.)			
	Residual Deviance:	464.05 (76 d.f.)			
	AIC:	879.25			
B. Model for pH and temperature experiment:	(Intercept)	−20.83	0.89	−23.37	***
y = pH + Temp. Group + pH * Temp. Group + e	pH	2.67	0.12	22.46	***
	High Temp.	16.75	1.13	14.88	***
	pH x High Temp	−2.13	0.15	−14.15	***
	Null Deviance:	2829.6 (89 d.f.)			
	Residual Deviance:	1514.4 (86 d.f.)			
	AIC:	2023.00			

A. GLM model evaluation of pH and dissolved oxygen effects with 5.9 mg/l dissolved oxygen group as the reference (surface water) data and 1.9 mg/l group as the comparative hypoxic group. Both data are constant at 13 °C. **B**. GLM evaluation for pH and temperature dual stressor experiment with 9 °C group (upwelling) as the reference temperature and 18 °C data as the comparative group (ocean warming). y = proportional fertilization response; e = error term; DO = dissolved oxygen; Temp. = temperature; * = $p < 0.05$; ** = $p < 0.01$; *** = $p < 0.001$.

that lower pH alters sperm swimming behavior and or sperm kinetics, ultimately negatively affecting fertilization outcomes. For example, a reduction of sperm swimming speed and percent motility was found to be significantly correlated with reduced fertilization success for *H. erythrogramma* at a pH level of 7.7 (Havenhand *et al.*, 2008). However, these results become confounding when compared with the negligible effects of pH reported by Byrne *et al.* (2010) for the same species and therefore, indicate that fertilization processes may be more complex. For example, changes in pH may also affect sperm attractant chemicals released by eggs (Riffell *et al.*, 2002), the activation process during egg fertilization via interference of lysine dissolution of the egg membrane (Kresge *et al.*, 2001), or the increase in H+ may ionically interfere with the explosive wave of calcium necessary for signalling egg activation and initiation of mitotic division (reviewed by Whitaker, 2006). Thus, while there is evidence for negative effects of low pH on fertilization success, the underlying physical or biological mechanisms require further evaluation—e.g. via biochemical tracing experiments—to fully understand when pH induces negative versus resistant outcomes.

The ameliorating effect of warming over the negative effects of pH below a threshold point has not been previously reported in invertebrate fertilization studies but this may be due to differences in our experimental design relative to prior studies. For example, in order to evaluate the effects of changing temperature and pH, Byrne *et al.* (2010) examined fertilization success with a 4-degree warming from ambient (∼20°C) coupled with 0.6 U decrease in pH from ambient (8.2 pH) for the tropical abalone *H. coccoradiata* and a 6-degree warming from ambient (∼20°C) coupled with 0.6 U decrease in pH from ambient (8.2 pH) for several species of echinoids. Under these conditions, fertilization success was found to be resistant to both drivers and without apparent interaction—i.e. fertilization rates remained high under all conditions. *Haliotis coccoradiata* and the echinoids examined by Byrne *et al.* (2010) are distributed at latitudes where near-shore temperatures average ∼20°C and where optimal fertilization success in these organisms have demonstrated to be ∼20°C (Wong *et al.*, 2010) and as such, an experimental temperature exposure of 18–26°C may not adequately capture the interactive effects of warming temperature and lower pH. That is, an ameliorating effect may be only observed if the experimental treatments include both warming and cooling comparisons of the same magnitude from the optimal temperature in combination with a fuller range of pH. Thus, experiments that examine co-variates moving in both directions from the optimal may reveal different patterns of multiple driver effects.

The negligible effect of low DO or hypoxia on fertilization observed in this study was unexpected. Oxygen is a critical driver of metabolic processes at multiple organismal scales. As oxygen is the terminal electron acceptor during mitochondrial energy production, loss of available oxygen would be expected to reduce the metabolic energy needed for flagellum activity or sperm propulsion. Thus, a reduction in sperm motility is expected to have negative consequences for sperm:egg interactions and ultimately fertilization success. For example, low levels of DO have been reported to reduce sperm swimming kinetics in marine species (Shin *et al.*, 2014; Graham *et al.*, 2016). However, as the overall role of oxygen in the metabolism involves creating a proton gradient, a decrease in seawater pH, or related changes in seawater carbonate parameters, may disrupt this proton gradient, or the effects of pH may dominate any effects of oxygen variation, at least over the scales examined. Indeed, Graham *et al.* (2016) observed an increase in the swimming speed of sea urchin sperm under lower pH and hypoxic conditions. However, despite the antagonistic interactive effects of pH and hypoxia on sperm motility, they also observed a synergistic decrease in fertilization under these combined drivers. Those results differ from our findings and may be indicative of differing species-specific responses. Furthermore, seawater conditions to which our adult brooders were acclimated to during reproductive development—which we did not characterize—may also influence fertilization outcomes. Negative impacts of seawater conditions during this phase are unlikely because the aquaculture tanks are highly aerated and the brooders are cultured separately and under low densities to minimize oxidative stress (Boch, pers. commun. with American Abalone Farms). Thus, while it may be possible that the effects of seawater pH may be greater than the effects of DO, future experiments

Table 3. Break-Point estimation.

A. Ocean acidification and hypoxia (all data)				
Segmented model	$y = \text{pH} + \text{U} + \text{psi} + e$			
	Estimate	**SE**	***z*-value**	***p*-value**
(Intercept)	−32.78	1.68	−19.55	***
pH	4.28	0.23	18.85	***
U	−3.10	0.47	−6.67	NA
Null seviance:	1316.42 (79 d.f.)			
Residual deviance:	413.25 (76 d.f.)			
AIC:	828.46			
Segmented model BP estimate	***7.56 ± 0.03 SE***			
Davies test BP estimate	***7.56****			
	Estimate	**SE**	**LCI (95%)**	**UCI (95%)**
Slope segment 1	***4.29***	0.23	3.83	4.74
Slope segment 2	***1.18***	0.41	0.37	1.99
B. Ocean acidification and warming (9 C dataset)				
Segmented model	$y = \text{pH} + \text{U} + \text{psi} + e$			
	Estimate	**SE**	***z*-value**	***p*-value**
(Intercept)	−35.62	2.20	−16.19	***
pH	4.69	0.30	15.69	***
U	−4.13	0.49	−8.36	NA
Null deviance:	1094.28 (44 d.f.)			
Residual deviance:	495.05 (41 d.f.)			
AIC:	748.04			
Segmented model BP estimate	***7.52 ± 0.02 SE***			
Davies test BP estimate	***7.52****			
	Estimate	**SE**	**LCI (95%)**	**UCI (95%)**
Slope segment 1	***4.69***	0.30	4.08	5.29
Slope segment 2	***0.56***	0.39	−0.24	1.35
C. Ocean acidification and warming (18 C dataset)				
Segmented model	$y = \text{pH} + \text{U} + \text{psi} + e$			
	Estimate	**SE**	***z*-value**	***p*-value**
(Intercept)	−2.44	1.01	−2.41	*
pH	0.32	0.14	2.33	*
U	1.69	0.71	2.39	NA
Null deviance:	977.09 (44 d.f.)			
Residual deviance:	933.94 (41 d.f.)			
AIC:	1197.5			
Segmented model BP estimate	***7.72 ± 0.06 SE***			
Davies test BP estimate	***7.73****			
	Estimate	**SE**	**LCI (95%)**	**UCI (95%)**
Slope segment 1	***0.32***	0.14	0.04	0.6
Slope segment 2	***2.01***	0.70	0.61	3.42

For each experiment, data are evaluated according to Table 2 GLM results with Segmented Model regression and Davies Test Breaking-Point estimation (Muggeo, 2008). **A**. Results for ocean acidification + hypoxia experiment data evaluated as a single dataset. **B**. Results for ocean acidification + 9 °C experiment data evaluated as an independent dataset. **C**. Results for ocean acidification + 18 °C experiment data evaluated as an independent dataset. U = difference in slopes of the two segments; psi = breaking point estimate at each step with standard error; e = error term; BP = Breaking Point; S.E. = ± standard error; NA = Not Applicable. LCI = Lower Confidence Interval; UPI = Upper Confidence Interval; * = $p < 0.05$; ** = $p < 0.01$; *** = $p < 0.001$.

should control for conditions during reproductive development to limit pre-existing exposures and to clarify experimental outcomes.

Prevailing theory based on aerobic scope suggests that exposure to anomalously high temperature and a secondary driver such as decreasing pH conditions would have a synergistic or an additive effect on fertilization success—i.e. dual stressors are predicted to narrow the window of biological performance (Portner and Farrell, 2008). However, our study shows that the effects of pH can be dominant over a secondary stressor such as hypoxia and in addition, the effects of ocean warming can ameliorate the effects of decreasing pH for fertilization success. Furthermore, it is unclear how warming temperatures in combination with hypoxic exposure may affect fertilization success. Altogether, our experimental results suggest that a synergistic or an additive response may not adequately describe the full scope of biological performance under multiple drivers or stressors—at least in the context of fertilization success. Based on our and other experimental studies on multiple environmental drivers, we instead suggest that the effects of multiple drivers can be complex and lead to resistance, dominance or amelioration. Importantly, our results show that non-linear responses and thresholds can also occur, highlighting the need to examine biological responses across continuous stressor gradients.

Understanding the influence of multiple co-varying environmental factors on the success of red abalone populations or similar marine organisms with complex life cycles requires that we disentangle the individual and combined effects of variation in key environmental drivers. In addition, it requires an understanding of the net outcomes that integrate the vulnerability of each life history stage. For example, although we found that fertilization rates increased with higher temperatures and decreased with upwelling-like conditions, *H. rufescens* have been found to have higher gonadal development under cooler phases of the California current (Vilchis *et al.*, 2005). Furthermore, male abalone exhibited a significant reduction of sperm production after 6 months of exposure to 18°C (Rogers-Bennett *et al.*, 2010). Thus, if abalone populations, which have been observed to be gravid from a few months to year-round (Boolootian *et al.*, 1962) respond to selection from the positive, negative, and other effects of environmental variation on gamete production and fertilization, the net demographic outcome may either be lessened or amplified by the ensemble of environmental drivers acting differentially on each life stage.

Our integrated approach to examine the effects of multiple environmental drivers provide new insights concerning the expected consequences of future changes in ocean conditions for abalone populations that were unlikely to be detected in single factor experiments. For the CCLME, our results suggest that red abalone fertilization success is at a possible tipping point under current upwelling events—i.e. 7.5 pH and 9–13°C. Our results also suggest that the effects could be further detrimental to fertilization success if ocean acidification causes a further reduction in seawater pH below 7.5. As gaps in our understanding remain, expanding integrated approaches will be critical to disentangle the effects of climate change and natural variability in multiple environmental drivers as we endeavor to predict and manage changes in marine populations.

Supplementary data

Supplementary material is available at the *ICESJMS* online version of the manuscript.

Acknowledgements

We are grateful to Kurt Buck, Patrick Whaling, Dale Graves, Joshua Lord, Jody Beers, Peter Hain, Tom Ebert, and numerous volunteers who helped with the experiments.

Funding

This study was supported by the US NSF-OA Programme (award no. OCE-1416934) and through the US NSF-CNH Programme (award no. DEB-1212124), and support from the David and Lucile Packard Foundation.

References

Babcock, R., and Keesing, J. 1999. Fertilization biology of the abalone *Haliotis laevigata*: laboratory and field studies. Canadian Journal of Fisheries and Aquatic Sciences, 56: 1668–1678.

Baker, M. C., and Tyler, P. A. 2001. Fertilization success in the commercial gastropod *Haliotis tuberculata*. Marine Ecology Progress Series, 211: 205–213.

Bakun, A. 1990. Global climate change and intensification of coastal upwelling. Science, 247: 198–201.

Bakun, A., Black, B. A., Bograd, S. J., García-Reyes, M., Miller, A. J., Rykaczewski, R. R., and Sydeman, W. J. 2015. Anticipated effects of climate change on coastal upwelling ecosystems. Current Climate Change Report, 1: 85–93.

Barros, P., Sobral, P., Range, P., Chicharo, L., and Matias, D. 2013. Effects of sea-water acidification on fertilization and larval development of the oyster *Crassostrea gigas*. Journal of Experimental Marine Biology and Ecology, 440: 200–206.

Barry, J. P., Lovera, C., Okuda, C., Nelson, E., and Pane, E. 2008. A gas-controlled aquarium system for ocean acidification studies. OCEANS 2008 – MTS/IEEE Kobe Techno-Ocean, Kobe. pp. 1–5.

Bograd, S. J., Castro, C. G., Di Lorenzo, E., Palacios, D. M., Bailey, H., Gilly, W., and Chavez, F. P. 2008. Oxygen declines and the shoaling of the hypoxic boundary in the California Current. Geophysical Research Letters, 35: L12607.

Boolootian, R. A., Farmanfarmaian, A., and Giese, A. C. 1962. On the reproductive cycle and breeding habits of two western species of Haliotis. Biological Bulletin, 122: 183–193.

Booth, J. A. T., McPhee-Shaw, E. E., Chua, P., Kingsley, E., Denny, M., Phillips, R., Bograd, S. J., *et al.* 2012. Natural intrusions of hypoxic, low pH water into nearshore marine environments on the California coast. Continental Shelf Research, 45: 108–115.

Byrne, M., Soars, N. A., Ho, M. A., Wong, E., McElroy, D., Selvakumaraswamy, P., Dwojanyn, S. A., and Davis, A. R. 2010. Fertilization in a suite of coastal marine invertebrates from SE Australia is robust to near-future ocean warming and acidification. Marine Biology, 157: 2061–2069.

Byrne, M. 2011. Impact of ocean warming and ocean acidification on marine invertebrate life history stages: vulnerabilities and potential for persistence in a changing ocean. Oceanography and Marine Biology: An Annual Review, 49: 1–42.

Cai, W., Borlace, S., Lengaigne, M., Van Rensch, P., Collins, M., Vecchi, G., Timmermann, A., *et al.* 2014. Increasing frequency of extreme El Nino events due to greenhouse warming. Nature Climate Change, 4: 111–116.

Caldeira, K., and Wickett, M. E. 2003. Anthropogenic carbon and ocean pH. Nature, 425: 365.

Chan, F., Barth, J. A., Lubchenco, J., Kirincich, A., Weeks, H., Peterson, W. T., and Menge, B. A. 2008. Emergence of anoxia in the California Current Large Marine Ecosystem. Science, 319: 920.

Connolly, T. P., Hickey, B. M., and Cochian, W. P. 2010. Processes influencing seasonal hypoxia in the northern California Current System. Journal of Geophysical Research, 115: C03021.

Crain, C. M., Kroeker, K., and Halpern, B. S. 2008. Interactive and cumulative effects of multiple human stressors in marine systems. Ecology Letters, 12: 1304–1315.

Deutsch, C., Brix, H., Ito, T., Franzel, H., and Thompson, L. 2011. Climate-forced variability of ocean hypoxia. Science, 333: 336–338.

Feely, R. A., Sabine, C. L., Lee, K., Berelson, W., Kleypas, J., Fabry, V. J., and Millero, F. J. 2004. Impact of anthropogenic CO_2 on the $CaCO_3$ system in the oceans. Science, 305: 362–366.

Feely, R. A., Sabine, C. L., Hernandez-Ayon, J. M., Ianson, D., and Hales, B. 2008. Evidence for upwelling of corrosive "acidified" water onto the Continental Shelf. Science, 320: 1490–1492.

Frieder, C. 2014. Present-day nearshore pH differentially depresses fertilization in congeneric species. Biological Bulletin, 226: 1–7.

Gattuso, J. P., Magnan, A., Bille, R., Cheung, W. W. L., Howes, E. L., Joos, F., Allemand, D., *et al.* 2015. Contrasting futures for ocean and society from different anthropogenic CO_2 emissions scenarios. Science, 349: aac4722.

Gazeau, F., Parker, L. M., Comeau, S., Gattuso, J. P., and O'Connor, W. A. 2013. Impacts of ocean acidification on marine shelled molluscs. Marine Biology, 160: 2207–2245.

Graham, H., Rastrick, S. P. S., Findlay, H. S., Bentley, M. G., Widdicombe, S., Clare, A. S., and Caldwell, G. S. 2016. Sperm motility and fertilization success in an acidified and hypoxic environment. 73: 783–790.

Halpern, B. S., McLeod, K. L., Rosenberg, A. A., and Crowder, L. B. 2008. Managing for cumulative impacts in ecosystem-based management through ocean zoning. Ocean and Coastal Management, 51: 203–211.

Havenhand, J. N., Buttler, F. R., Thorndyke, M. C., and Williamson, J. E. 2008. Near-future levels of ocean acidification reduce fertilization success in a sea urchin. Current Biology, 18: R651–R652. doi:10.1016/jcub.2008.06.2015.

Huchette, S. M. H., Soulard, J. P., Koh, C. S., and Day, R. W. 2004. Maternal variability in the blacklip abalone, *Haliotis rubra* leach (Mollusca: Gastropoda): effect of egg size on fertilization success. Aquaculture, 231: 181–195.

Keeling, R. F., Kortzinger, A., and Gruber, N. 2010. Ocean deoxygenation in a warming world. Annual Review of Marine Science, 2: 199–229.

Kim, T. W., Barry, J. P., and Micheli, F. 2013. The effects of intermittent exposure to low-pH and low-oxygen conditions on survival and growth of juvenile red abalone. Biogeosciences, 10: 7255–7262.

Kresge, N., Vacquier, V. D., and Stout, C. D. 2001. Abalone lysine: the dissolving and evolving sperm protein. BioEssays 23: 95–103.

Kroeker, K. J., Kordas, R. L., Crim, R. N., and Singh, G. G. 2010. Meta-analysis reveals negative yet variable effects of ocean acidification on marine organisms. Ecology Letters, 13: 1419–1434.

Kroeker, K. J., Kordas, R. L., Crim, R., Hendriks, I. E., Ramos, L., Singh, G. S., Duarte, C. M., and Gattuso, J. P. 2013. Impacts of ocean acidification on marine organisms: quantifying sensitivities and interaction with warming. Global Change Biology, 19: 1884–1896.

Kurihara, H., and Shirayama, Y. 2004. Effects of increased atmospheric CO_2 on sea urchin early development. Marine Ecology Progress Series, 274: 161–169.

Lee, T., and McPhaden, J. 2010. Increasing intensity of El Niño in the central-equatorial Pacific. Geophysicla Research Letter, 37: L14603.

Micheli, F., Saenz-Arroyo, A., Greenley, A., Vazquez, L., Montes, J. A. E., Rossetto, M., and De Leo, G. A. 2012. Evidence that marine reserves enhance resilience to climatic impacts. PLoS One, 7: e40832.

Morse, D. E., Duncan, H., Hooker, N., and Morse, A. 1977. Hydrogen peroxide induces spawning in mollusks, with activation of prostaglandin endoperoxide synthase. Science, 196: 298–300.

Moulin, L., Catarino, A. I., Claessens, T., and Dubois, P. 2011. Effects of seawater acidification on early development of the intertidal sea urchin *Paracentrotus lividus* (Lamarck 1816). Marine Pollution Bulletin, 62: 48–54.

Muggeo, V. M. R. 2003. Estimating regression models with unknown break-points. Statistics in Medicine, 22: 3055–3071.

Muggeo, V. M. R. 2008. Segmented: an R package to fit regression models with Broken-Line Relationships. R News, 8/1: 20–25.

Orr, J. C., Fabry, V. J., Aumont, O., Bopp, L., Doney, S. C., Feely, R. A., Gnanadesikan, A., *et al.* 2005. Anthropogenic ocean acidification over the twenty-first century and its impact on calcifying organisms. Nature, 437: 681–686.

Portner, H. O., and Farrell, A. P. 2008. Physiology and climate change. Science, 322: 690–692.

Riffell, J. A., Krug, P. J., and Zimmer, R. K. 2002. Fertilization in the sea: the chemical identity of an abalone sperm attractant. The Journal of Experimental Biology, 205: 1439–1450.

Rogers-Bennett, L., Dondanville, R. F., Moore, J. D., and Vilchis, L. I. 2010. Response of red abalone reproduction to warm water, starvation, and disease stressors: implications of ocean warming. Journal of Shellfish Research, 29: 599–611.

Sabine, C. L., Feely, R., Gruber, N., Key, R. M., Lee, K., Bullister, J. L., Wanninkhof, R., *et al.* 2004. The oceanic sink for anthropogenic CO_2. Science, 305: 367–371.

Scanes, E., Parker, L. M., O'Connor, W. A., and Ross, P. M. 2014. Mixed effects of elevated pCO_2 on fertilization, larval and juvenile development and adult responses in the mobile subtidal scallop *Mimachlamys asperrima* (Lamarchk, 1819). PLoS One, 9: e93649. doi:10.1371/journal.pone.0093649

Shepherd, S. A., Turrubeates-Morales., and Hall, K. 1998. Decline of the abalone fishery at La Natividad, Mexico: Overfishing or climate change? Journal of Shellfish Research, 17: 839–846.

Shin, P. K. S., Leung, J. Y. S., Qiu, J. W., Ang, P. O., Chiu, J. M. Y., Thiyagarajan, V., and Cheung, S. G. 2014. Acute hypoxic exposure affects gamete quality and subsequent fertilization success and embryonic development in a serpulid polychaete. Marine Pollution Bulletin, 85: 439–445.

Solomon, S., Qin, D., Manning, M., Chen, Z., Marquis, M., Avery, K. B., Tigonor, M., and Miller, H. L. Eds. 2007. Contribution of Working Group I to the Fourth Assessment Report of the Intergovernmental Panel on Climate Change. Cambridge University Press, Cambridge, United Kingdom and New York, NY, USA.

Somero, G. N., Beers, J. M., Chan, F., Hill, T. M., Klinger, T., and Litvin, S. Y. 2016. What changes in the carbonate system, oxygen, and temperature portend for the Northeastern Pacific Ocean: A physiological perspective. BioScience, 66: 14–26.

Stramma, L., Schmidtko, S., Levine, L., and Johnson, G. C. 2010. Ocean oxygen minima expansions and their biological impacts. Deep-Sea Research I, 57: 587–595.

Sydeman, W. J., Garcia-Reyes, M., Schoeman, D. S., Rykaczewski, R. R., Thompson, S. A., Black, B. A., and Bograd, S. J. 2014. Climate change and wind intensification in coastal upwelling ecosystems. Science, 345: 77–80.

Trenberth, K. E., and Hoar, T. J. 1997. El Niño and climate change. Geophysical Research Letters, 24: 3057–3060.

Vaquer-Sunyer, R., and Duarte, C. M. 2008. Thresholds of hypoxia for marine biodiversity. Proceedings of the National Academy of Sciences of the United States of America, 105: 15452–15457.

Vilchis, L. I., Tegner, M. J., Moore, J. D., Friedman, C. S., Riser, K., Robbins, T. T., and Dayton, P. K. 2005. Ocean warming effects on growth, reproduction, and survivorship of southern California abalone. Ecological Applications, 15: 469–480.

Walter, R. K., Woodson, C. B., Leary, P. R., and Monismith, S. G. 2014. Connecting wind-driven upwelling and offshore stratification to nearshore internal bores and oxygen variability. Journal of Geophysical Research Oceans, 119: 3517–3534.

Warton, D. I., and Hui, F. K. C. 2011. The arcsine is asinine: the analysis of proportions in ecology. Ecology, 92: 3–10.

Whitaker, M. 2006. Calcium at fertilization and in early development. Physiology Review, 86: 25–88.

Wong, E., Davis, A. R., and Byrne, M. 2010. Reproduction and early development in Haliotis coccoradiata (Vetigastropoda: Haliotida). e. Invertebrate Reproduction and Development, 54: 77–87.

Handling editor: David M. Fields